

CMS Conference Report

December 19, 2001

Higgs Physics at the LHC

K. Lassila-Perini

Helsinki Institute of Physics

Abstract

The physics of the Higgs sector in the Standard Model and the Minimal Supersymmetric Standard Model at the LHC is reviewed. The Higgs discovery reach of the two general-purpose experiments, ATLAS and CMS, is summarised.

Presented at *III International Symposium on LHC Physics and Detectors*, Chia, October 25–27, 2001

Submitted to *EPJdirect*

1 Introduction

The Standard Model[1] of strong and electroweak interactions is in excellent agreement with the experimental measurements. However, the core of the theory, the electroweak symmetry breaking manifesting itself in the heavy vector bosons W and Z and the massless photon, is the least known sector of the model. The Higgs mechanism[2] provides a mathematical explanation to this phenomenon, and one of the main tasks of the LHC collider will be the quest for experimental evidence of the Higgs particle, or any observable of some other symmetry breaking mechanism.

In this note, the Higgs sectors of the Standard Model and the Minimal Supersymmetric Standard Model are reviewed. The production mechanism at the LHC are briefly discussed as well as the possible decay modes. The discovery potential of the two general-purpose detectors ATLAS[3] and CMS[4] are summarised without going into details of the detector performance or trying to compare the individual performance of the two detectors. The possible precision measurements of the Higgs particle are briefly mentioned and the note concludes with two hypothetical visions after the first 10 fb^{-1} , the integrated luminosity which is foreseen after the first physics run of the LHC collider in 2007.

2 What are we looking for?

Without the Higgs boson the Standard Model is neither consistent nor complete. It provides the remedy for the unitarity violation of the longitudinal gauge boson scattering at $\sqrt{s_{WW}} \gtrsim 1 \text{ TeV}$. The masses of the gauge bosons and fermions are generated through the interaction with the Higgs field.

2.1 The SM Higgs

The only unknown parameter in the SM Higgs sector is the mass of the Higgs boson. This is not predicted by the theory, but indirect constraints for the possible mass range can be deduced from theoretical arguments[5]. Furthermore, the electroweak precision measurements, where the Higgs mass enters in the radiative corrections, can be used to predict the most likely value of the Higgs mass consistent with all the experimental data used in the fit. Such fits favour a rather light Higgs boson, $m_H < 196 \text{ GeV}$ with 95% confidence level[6]. Experimentally, direct searches at LEP exclude the SM Higgs boson below $m_H = 114.1 \text{ GeV}$ at 95% confidence level[7].

The SM Higgs would be the first fundamental scalar particle. It has the nice features of allowing the spontaneous symmetry breaking giving gauge bosons their masses and it also provides fermions their masses through Yukawa couplings. However, when the bare mass of this scalar particle is computed in the perturbation theory, it turns out that the mass diverges quadratically. Technically, this problem could be solved by renormalization, resulting in a counter-term balancing the quadratic divergence in each order of the perturbative calculations, but such fine-tuning cannot be considered natural or elegant. This unpleasant feature of the SM is one of the main motivations to search for a theory without such a drawback.

2.2 The MSSM Higgs

In supersymmetric theories[8], for each SM particle a supersymmetric partner is introduced. These *sparticles* have the same quantum numbers as the particles but their spin differs by one half. The introduction of the supersymmetric partners cancels the quadratic divergence in the Higgs boson mass, thus solving the fine-tuning problem, provided the masses of the supersymmetric partners are not beyond 1 TeV scale.

In this note, we concentrate on the Minimal Supersymmetric extension[9] of the Standard Model, which is minimal in the sense that a minimum number, i.e. two, of Higgs doublets is introduced. This results in five observable Higgs particles in the MSSM: two neutral CP-even scalars, a light h and a heavy H, a CP-odd A, and charged H^+ and H^- . In the MSSM, at tree level, the Higgs sector is defined by two parameters which can be chosen to be the mass of the CP-odd A, m_A , and $\tan \beta$, the ratio of the vacuum expectation values of the two Higgs doublets. There are other parameters which effect the Higgs sector through radiative corrections, such as the top quark mass, the mass scales of the SUSY particles and the mixing between the left and right handed components of the stop squark.

The two parameters, m_A and $\tan \beta$, define the masses of other Higgs particles as shown in figure 1[10] for the maximal mixing of the stop squark mass. The light h reaches its maximal mass already at moderate m_A values. This is the so called decoupling limit where the light h has the same couplings as in the SM, and this condition is true in a large area of the m_A - $\tan \beta$ parameter space. Above $m \approx 200 \text{ GeV}$ the heavy Higgses (H, A and H^\pm) are almost degenerate in mass. In the MSSM the Higgs masses are strongly correlated.

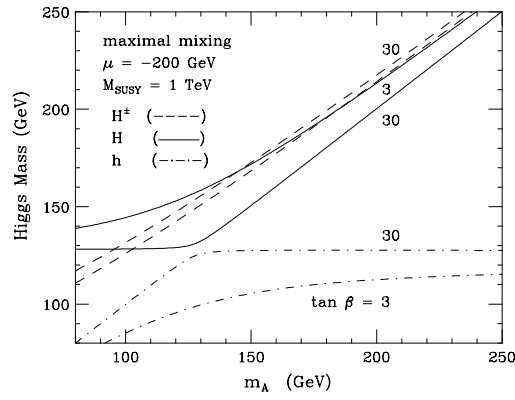


Figure 1: The masses of h , H and charged H as a function of m_A with different values of $\tan\beta$ [10].

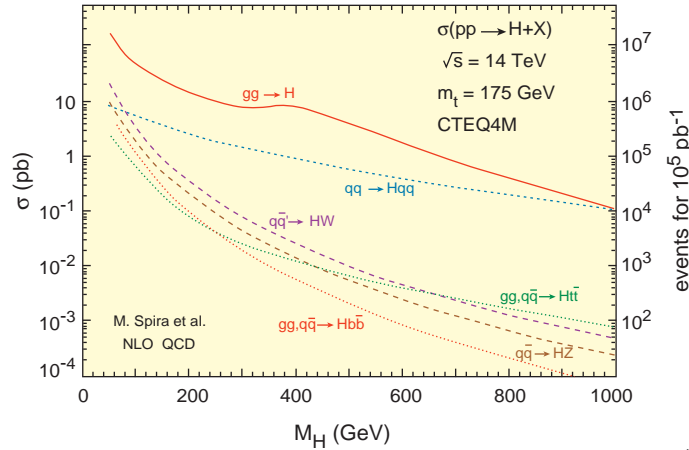


Figure 2: The Higgs production cross-sections[12] as a function of m_H at the LHC.

The LEP experiments have excluded a light h below 91 GeV, an A below 91.9 GeV and a charged Higgs below 78.6 GeV[11]. For maximal stop mixing the range $0.5 < \tan\beta < 2.4$ has been excluded, and for minimal mixing $0.7 < \tan\beta < 10.5$ [11]. In this note, most of the examples are given for the maximal mixing scenario as this is considered to be the most difficult case at the LHC.

3 What is going to be produced at the LHC?

In this section, Higgs production and decay at the LHC are reviewed. The cross-sections have been computed with the Higgs production programs HIGLU, VV2H, V2HV and HQQ[12] based on the calculations in [13] and the branching ratios have been computed with HDECAY[14].

3.1 Higgs production and decay in the SM

The most important Higgs production channel at the LHC will be the gluon-gluon fusion as shown in figure 2. It is the dominant production mechanism through all the Higgs mass range, and in 10 fb^{-1} , it results in some hundred thousand to a thousand Higgs events depending on the Higgs mass. At higher Higgs masses, the vector boson fusion channel gains importance. It is an interesting channel because the two quark lines result in two forward jets which can be used to tag the event and to reduce the background. In the same manner, $t\bar{t}$ fusion offers the possibility to tag the two top quarks.

Figure 3 shows the branching ratios of the different decay modes. The $b\bar{b}$ channel is the dominant decay up to the opening of the vector boson channels which then dominate. Figure 4 shows the rates of most of the observable

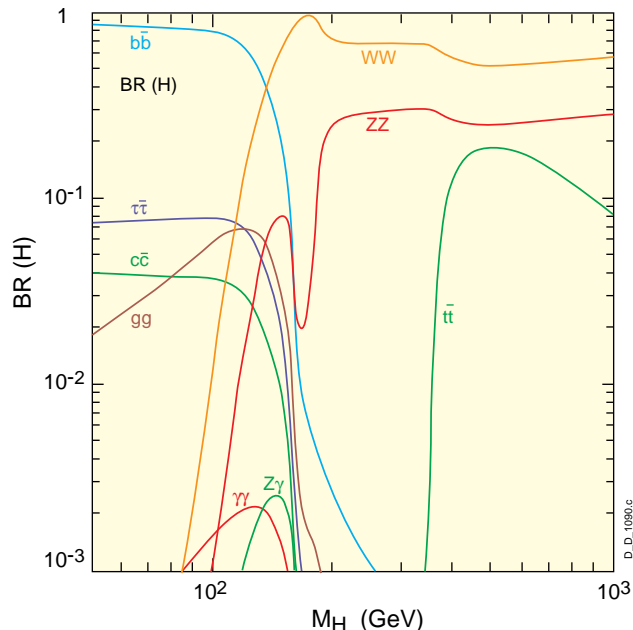


Figure 3: The Higgs branching ratios[14] as a function of m_H at the LHC.

Higgs decay final states. The continuous lines show the decay channels where all the final state products can be observed, and the dashed lines the channels where the final state includes some neutrinos. The most abundant channel in the figure is the $2\nu 2\ell$ decay of the WW pair. However, this final state offers only an excess of the events in the p_T distribution of the two leptons and the mass peak cannot be directly reconstructed. The $H \rightarrow \gamma\gamma$ channel results in some hundred events in 10 fb^{-1} up to $m_H \approx 150 \text{ GeV}$. The best channel, the ZZ decay in four leptons, has a lower rate but it extends up to high masses. To complete the figure, one should mention the $H \rightarrow b\bar{b}$ channel which offers very high rate at the lower masses.

3.2 Higgs production and decay in the MSSM

In the MSSM, the SM Higgs couplings are modified as a function of the angles β and α which is a function of m_A and β at tree level. The resulting cross-sections are shown with two values of $\tan\beta$ in figure 5 for h and H and in figure 6 for A . For comparison, the dominant SM process, the gluon-gluon fusion, is shown in the plots. It can be concluded that the total rate is suppressed or enhanced at low and high $\tan\beta$, respectively. The vector boson fusion is suppressed, for h and H especially at high $\tan\beta$, and altogether for A which does not couple to vector bosons at tree level. Higgs production in association with a $b\bar{b}$ pair is strongly enhanced and it becomes the dominant production mechanism at high $\tan\beta$.

The Higgs decay pattern can be extremely complicated as shown in figure 7 for h and H . For the light h , the branching ratios reach their SM value when m_h reaches its maximum value. It is worth noting that even if this area is just a narrow line when plotted as a function of m_h , it covers most of the m_A - $\tan\beta$ parameter plane. The decay into a $b\bar{b}$ pair is dominant for the light h with $m_h < m_{h,max}$ and for the heavy H at high $\tan\beta$. The decays into WW and ZZ pairs are suppressed, especially with rising $\tan\beta$. The $\tau\tau$ decay is enhanced. The SUSY parameters have been chosen so that the decay into $\chi^0\chi^0$ and $\chi^+\chi^-$ are possible. This illustrates how the SUSY parameters can affect the Higgs sector even if in most cases it remains quite decoupled from the rest of the model parameters.

Figure 8 shows the branching ratios for A . The $b\bar{b}$ decay is dominant and the $\tau\tau$ decay much more significant than in the SM where the opening of the vector boson channels suppresses the fermion decays. As illustrated in the plot, the decays to SUSY particle may be important if their masses are light enough.

The charged Higgs can be produced in the top quark decay if its mass is lighter than the top quark mass. If it is heavier, it is produced in other processes alone, or in association with a top quark or a tb quark pair. The branching ratios of H^\pm decays are shown in figure 9. The decay to a tb quark pair is dominant where kinematically possible. Below m_{top} mass, the $\tau\nu$ decay is dominant. The SUSY parameters chosen for the plot allow the decay to a chargino neutralino pair in the high mass range.

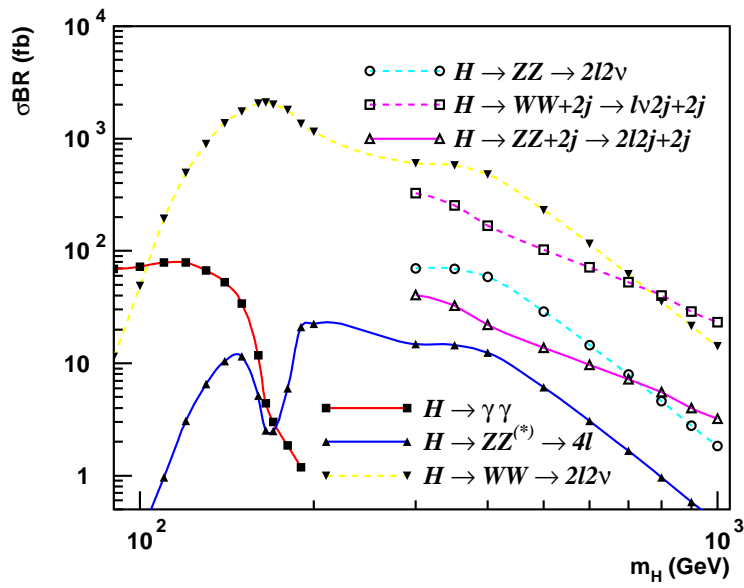


Figure 4: The Higgs production rates in different decay channels as a function of m_H at the LHC[15].

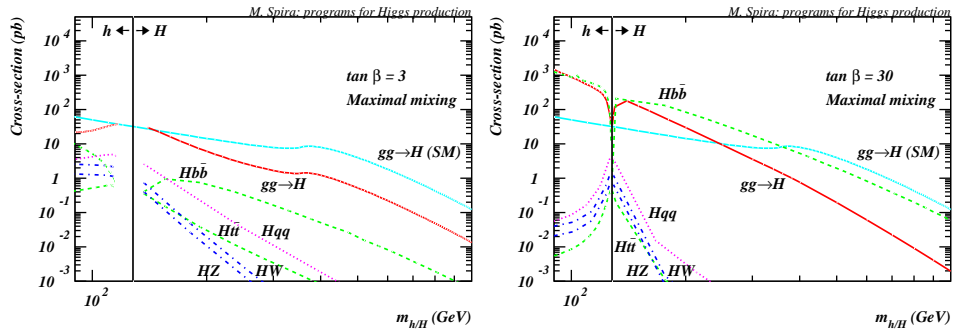


Figure 5: Higgs production cross-sections[12] of the light h and heavy H as a function of their masses.

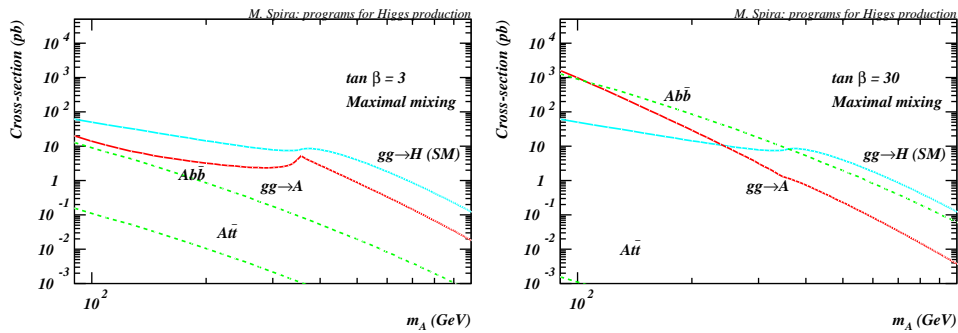


Figure 6: Pseudo-scalar Higgs production cross-sections[12] as a function of m_A .

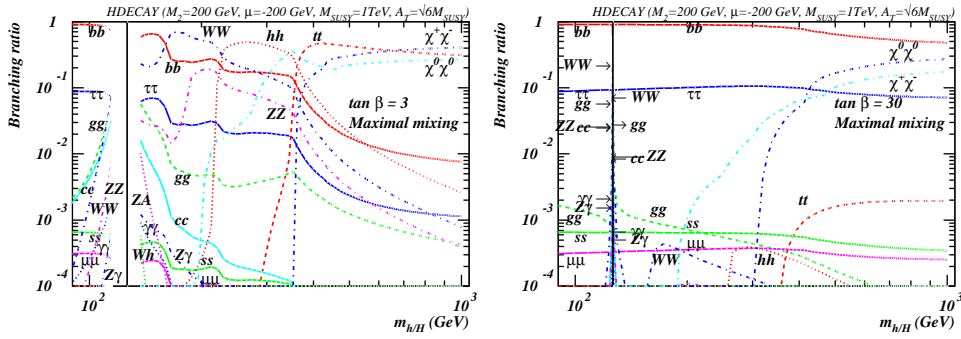


Figure 7: The branching ratios[14] of the light h and heavy H as a function of their masses.

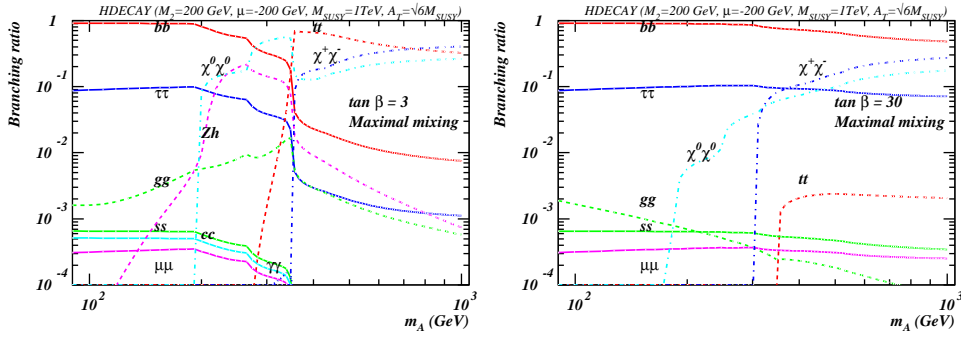


Figure 8: The branching ratios[14] of A as a function of m_A .

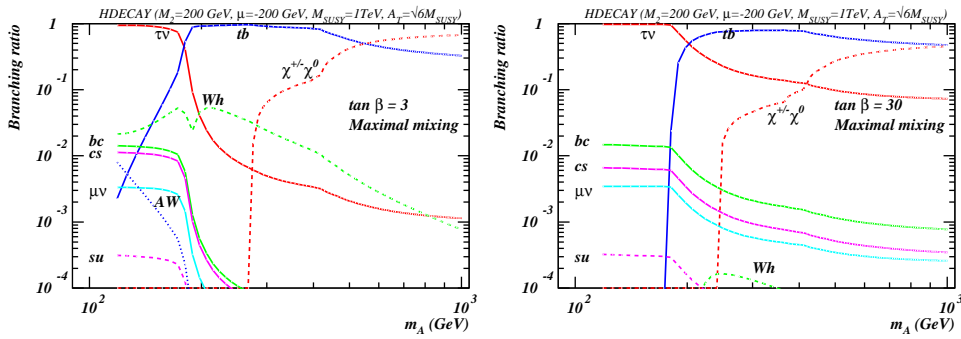


Figure 9: The branching ratios[14] of H^\pm as a function of m_{H^\pm} .

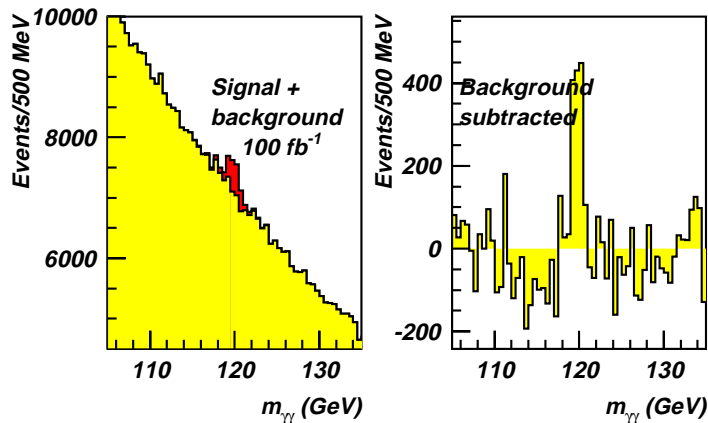


Figure 10: $H \rightarrow \gamma\gamma$ ($m_H = 120$ GeV) signal over the background and with the background subtracted in CMS with 100 fb^{-1} [15].

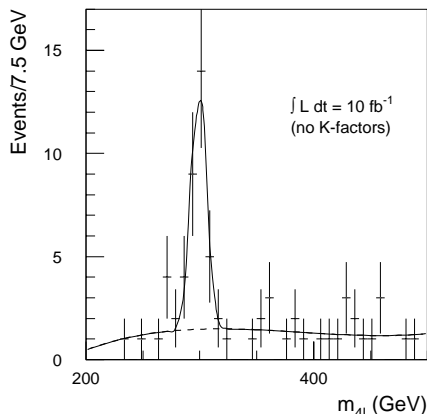


Figure 11: $H \rightarrow 4\ell$ ($m_H = 300$ GeV) signal over the background in ATLAS[16].

4 What do we expect to observe at the LHC?

One of the main goals of the LHC experiments is to assure that the Higgs boson can be discovered – or excluded – in the full parameter space. For the SM Higgs, we are prepared to cover the mass range from (and below) the LEP limits up to ≈ 1 TeV. In the MSSM, the aim is to cover the entire m_A - $\tan\beta$ plane. In this section, some examples of the main channels observable at the LHC are given and the discovery potential is summarised.

4.1 The SM Higgs

The SM offers two high precision discovery channels: the decay into two photons and the $ZZ^{(*)}$ decay into four leptons (electrons or muons). Figure 10 illustrates the reconstructed mass of a 120 GeV Higgs decaying into two photons in the CMS experiment with 100 fb^{-1} [15]. The significance of the signal is 10.3σ . The importance of the excellent photon efficiency and resolution is clearly visible, a worse resolution would flatten the signal events over the very large irreducible $\gamma\gamma$ background, thus degrading the visibility of the signal. Figure 11 shows the reconstructed mass of a 300 GeV Higgs decaying into four leptons in the ATLAS experiment in with 10 fb^{-1} [16]. The production rates are lower than for the two photon channel, but the background can be very effectively suppressed. A very clean signal with practically no background can be obtained already with a small integrated luminosity ($\lesssim 10 \text{ fb}^{-1}$).

The mass range up to 600 GeV can be covered with the two precision channels. In the lowest mass range ($90 \text{ GeV} < m_H \lesssim 130 \text{ GeV}$), the Higgs decay into a $b\bar{b}$ pair can be visible when the presence of the $t\bar{t}$ pair – from the Higgs production through $t\bar{t}$ fusion – is required, and one of the top quarks decays leptonically. The final state is thus $t\bar{t}H \rightarrow \ell\nu q\bar{q}b\bar{b}$ where one $b\bar{b}$ pair is the Higgs decay product, the two other b quarks come from the top quark

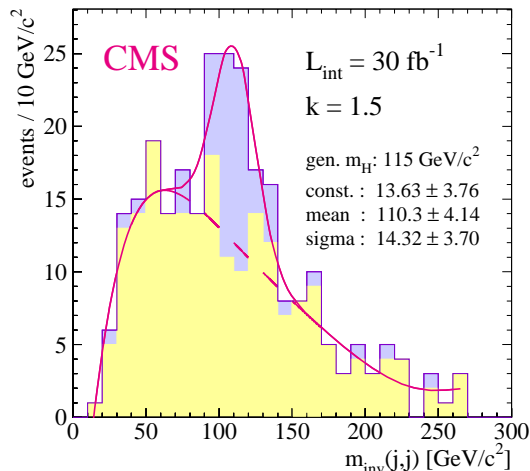


Figure 12: $H \rightarrow b\bar{b}$ ($m_H = 115$ GeV) signal over the background with 30 fb^{-1} in CMS[17].

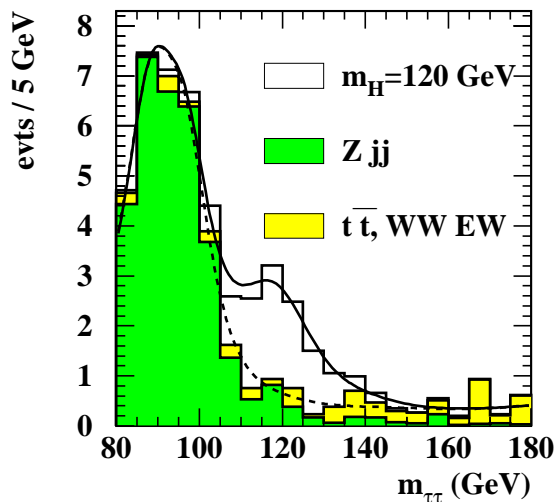


Figure 13: $H \rightarrow \tau\tau$ ($m_H = 120$ GeV) signal over the background with 30 fb^{-1} in ATLAS[19].

leptonic ($\ell\nu$) and hadronic ($q\bar{q}$) decays. This very complicated final state can be triggered due to the presence of the lepton, and the background can be reduced by b -tagging and fully reconstructing the top quark decays. Figure 12 shows the reconstructed mass of a 115 GeV Higgs decaying into b quarks for 30 fb^{-1} [17]. The background can be effectively suppressed and a clear 5.3σ signal is visible.

The inclusive $H \rightarrow WW \rightarrow 2\ell 2\nu$ and $H \rightarrow ZZ \rightarrow 2\ell 2\nu$ channels offer sensitivity over almost the full mass range. The WW channel complements the difficult region of the four lepton channel below the ZZ threshold, and will be the fastest discovery channel at $m_H \approx 170$ GeV, provided the backgrounds are well understood.

The vector boson fusion channels with the two forward tagging jets can be used to complete the high Higgs mass range. Furthermore, recent studies[18, 19] show that for example even the $H \rightarrow \tau\tau$ decay could be visible when the Higgs is produced through vector boson fusion. The reconstructed mass is shown in figure 13 for 30 fb^{-1} [19]. Requiring the two forward tags and making use of the clean central area of vector boson fusion events, the background to many channels can be efficiently suppressed, thus giving an opportunity for precision measurements in the absence of the background.

The SM Higgs discovery potential in the ATLAS experiment for 100 fb^{-1} is summarised in figure 14[16]. The full mass range can be covered with a large margin over the 5σ significance level and in most areas with more than one channel at a time. Figure 15[20] shows the minimum luminosity required to achieve a 5σ discovery in CMS. Already with 10 fb^{-1} , the mass range between 130 GeV and 600 GeV can be explored.

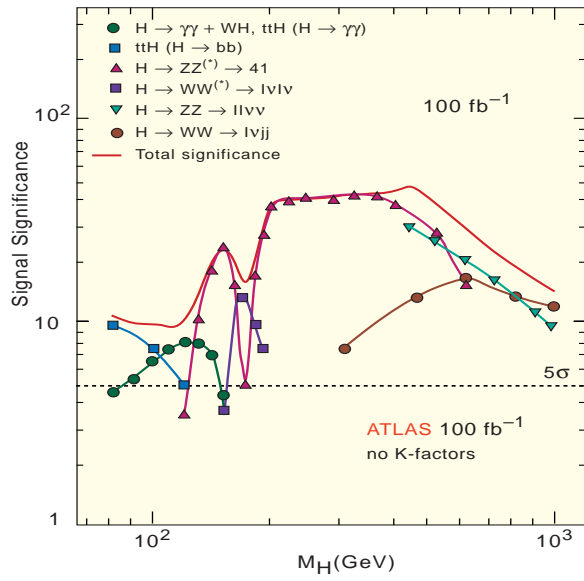


Figure 14: The discovery reach of the SM Higgs for 100 fb^{-1} in ATLAS[16].

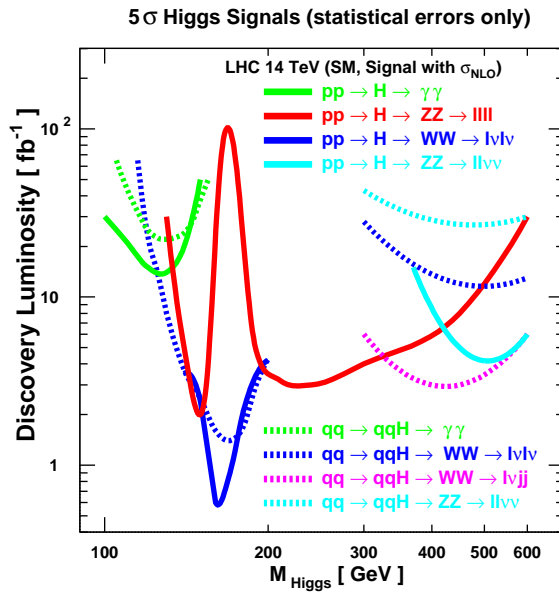


Figure 15: The minimum luminosity to reach 5σ discovery in CMS[20].

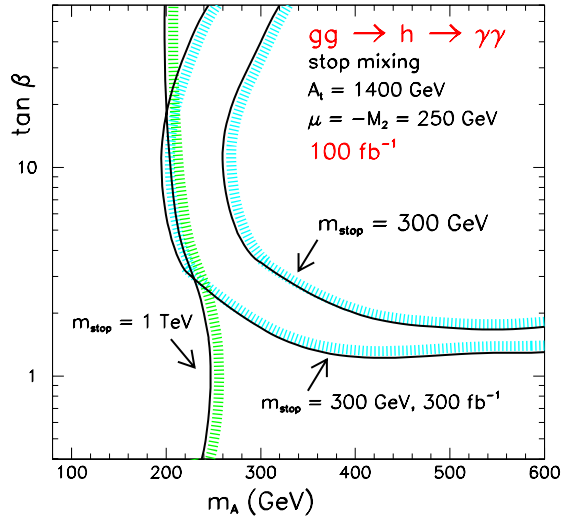


Figure 16: The expected 5σ reach for $h \rightarrow \gamma\gamma$ CMS[21].

4.2 The MSSM Higgses

Of the numerous MSSM decay modes, four channels are of major importance: $h \rightarrow \gamma\gamma$, $h \rightarrow b\bar{b}$, $H/A \rightarrow \tau\tau$ and $H^\pm \rightarrow \tau\nu$. These channels will be shortly discussed in the following. The best SM channel, $H \rightarrow ZZ \rightarrow 4l$ is strongly suppressed. There are several other channels to complete in different regions of the parameter space, such as heavy H or A decaying in light h, muonic decay of H or A and tb pair decay of the charged Higgs, to mention a few. Furthermore, if the SUSY mass scale allows the decay into SUSY particles the $H/A \rightarrow \chi_2^0\chi_2^0$ could be visible. The light h could also be produced in the neutralino decay $\chi_2^0 \rightarrow h\chi_1^0$.

The supersymmetric light h has production and decay modes as in the SM when m_h reaches its maximal value for a given $\tan\beta$. The two photon decay is suppressed below this mass but as $m_h = m_{h,max}$ above $m_A \approx 200$ GeV, this decay offers sensitivity in a large area of parameter space. Figure 16 shows the parameter space coverage for this channel in CMS[21]. For 100 fb^{-1} , the area above $m_A = 200 - 245$ GeV is covered in the case of the maximal stop mixing and when the mass scale of the lightest SUSY particle is in the 1 TeV range. This is the most common choice of parameters. It is worth noting, however, that the light h production through gluon-gluon fusion is very sensitive to the mass of the lightest SUSY particle[22]. If the stop mixing is maximal and the stop mass is chosen to be 300 GeV, the parameter space coverage is reduced, and the full $m_{stop} = 1$ TeV coverage cannot be recovered even with 300 fb^{-1} as indicated in figure 16. However, in that case, the h production in association with W or $t\bar{t}$ which proceeds through tree diagrams is unaffected and the $h \rightarrow \gamma\gamma$ decay in these channels can be used to restore the parameter space coverage.

The $h \rightarrow b\bar{b}$ decay has a large branching ratio over the whole parameter space and thus extends the reach of the light h discovery to the lower values of m_A . The decay has the same features as in the SM and the 5σ reach is shown in figure 17[24]. Only a small area at lowest m_A and highest $\tan\beta$ is left uncovered.

The $H/A \rightarrow \tau\tau$ decay[23] is the most important channel in the search for for the neutral heavy Higgses, and it is particularly significant at high $\tan\beta$. Experimentally, the τ decays are very interesting, they require an interplay of different detector elements measuring missing E_T due to the escaping neutrinos, leptons from the leptonic τ decay, jets from the hadronic τ decays and tracks for the b-tagging when the b quarks produced in association with the Higgs are required to suppress the background. The best significance for this channel is obtained choosing the H production in association with a $b\bar{b}$ pair. The event can be triggered with a specific τ trigger (or electron and muon trigger in case of the leptonic τ decay). The QCD background is effectively suppressed by the missing E_T cut. Furthermore, the leptonic τ decays can be identified with τ tagging using an impact parameter cut. The reconstructed mass in the $A/H \rightarrow \tau\tau \rightarrow e\mu + X$ channel is shown in figure 18[25]. The parameter space coverage for the heavy Higgs H and A is shown in figure 19[24]. The τ decay channels cover the high $\tan\beta$ part of the parameter space, and several other channels contribute, many of which however in the area already covered by LEP. The muonic decay of H and A is interesting as it allows a precise reconstruction of the mass peak and it could possibly allow the separation between H and A, almost degenerate in mass. The width of H and A as a function of

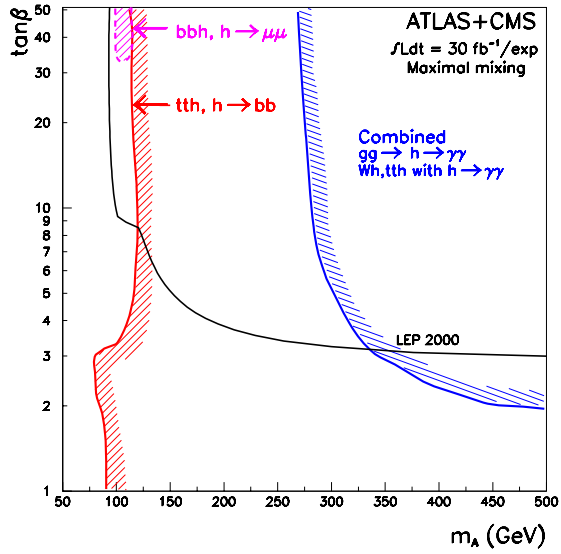


Figure 17: The expected 5σ reach for the light h combining 30 fb^{-1} per experiment[24].

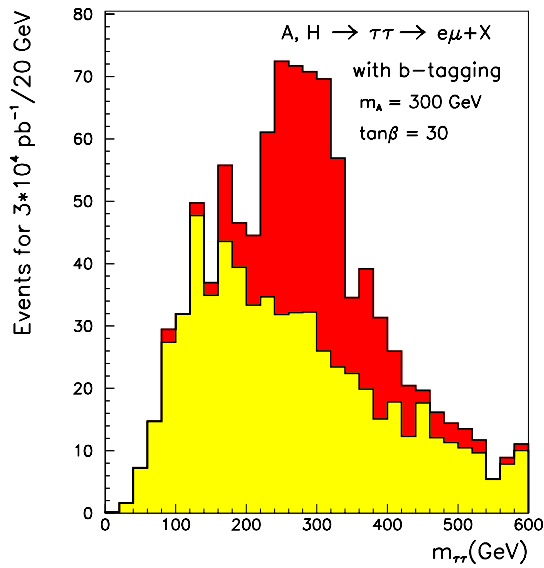


Figure 18: The reconstructed mass of $A/H \rightarrow \tau\tau \rightarrow e\mu + X$ over the background with 30 fb^{-1} in CMS[25].

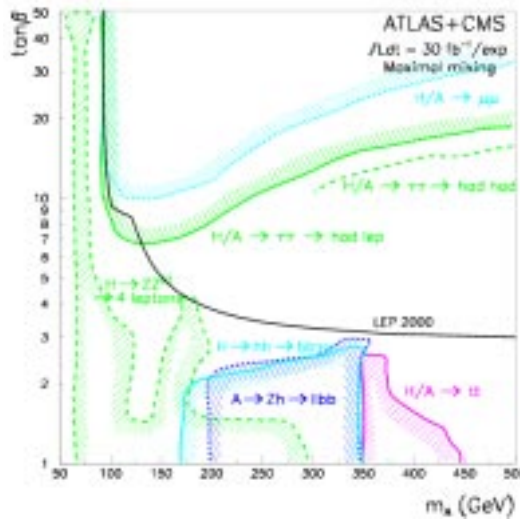


Figure 19: The expected 5σ reach for H and A combining 30 fb^{-1} per experiment[24].

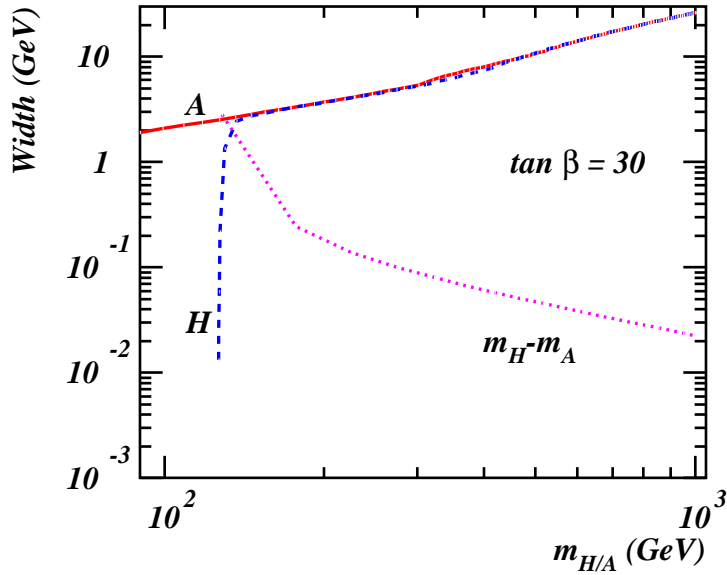


Figure 20: The width of the H and A boson as a function of m_A and the difference between m_A and m_H for $\tan\beta = 30$.

m_A and the difference between their masses at $\tan\beta = 30$ is shown in figure 20. For moderate values of m_A the separation between A and H is feasible.

The charged Higgs can be observed in the $t\bar{t}$ events if $m_H^\pm < m_{top}$ or in the decay into $\tau\nu$ when $m_H^\pm > m_{top}$ and H^\pm is produced in association with a top quark. Figure 21 shows the reconstructed transverse mass for $m_{H^\pm} = 400\text{ GeV}$ and 200 GeV with expected background for 100 fb^{-1} [26]. To obtain a clear separation between the signal and the background the τ polarisation properties has been exploited. The polarisation of a τ originating from a spin-0 Higgs is different than of a τ from a spin-1 vector bosons and the hadronic decay products of τ , in particular in $\tau \rightarrow \pi\nu$, are expected to be boosted into the τ direction. Furthermore, the W and the top mass are reconstructed, and the b -jet from the top quark decay is tagged.

Figure 22 summarises the expected 5σ discovery reach for 30 fb^{-1} for maximal stop mixing[21]. Almost all the parameter plane can be covered with the exception of a small area at low m_A and low $\tan\beta$. Many regions have several decay modes available, but in the low and intermediate values of $\tan\beta$ only the light h will be visible. Figure 23 illustrates – in a different scale – how the uncovered region can be covered summing together 30 fb^{-1} of

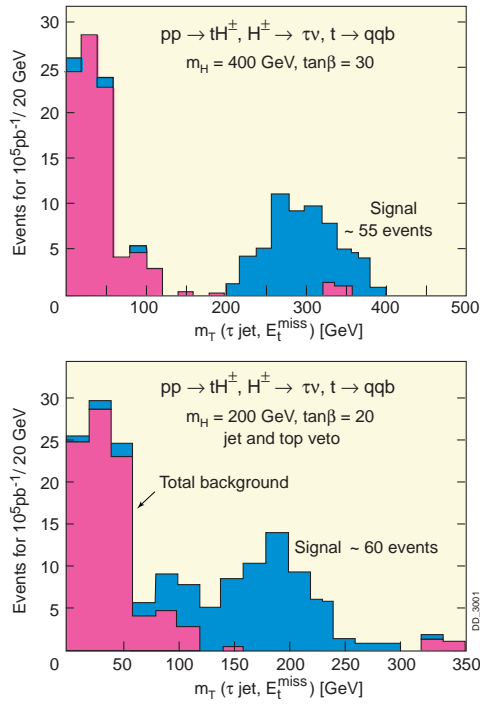


Figure 21: The reconstructed transverse mass of 400 GeV and 200 GeV H^\pm for $\tan\beta = 30$ and 20, respectively, over the background for 100 fb^{-1} in CMS[26].

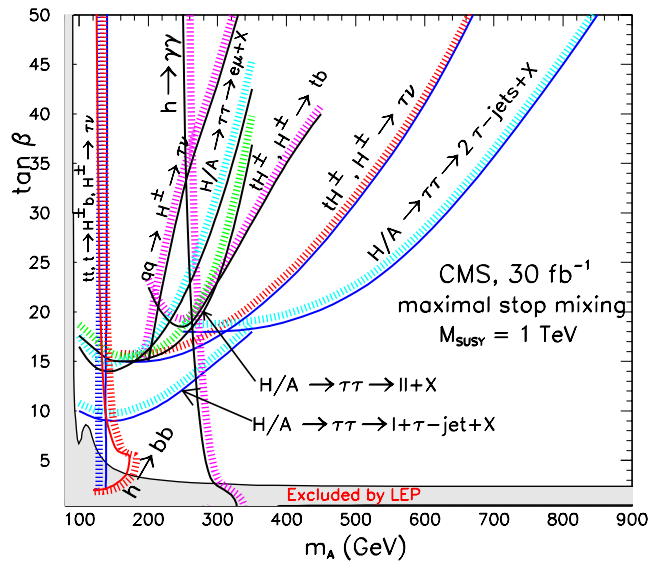


Figure 22: The expected 5σ discovery reach for MSSM Higgses for 30 fb^{-1} in case of maximal stop mixing in CMS[21].

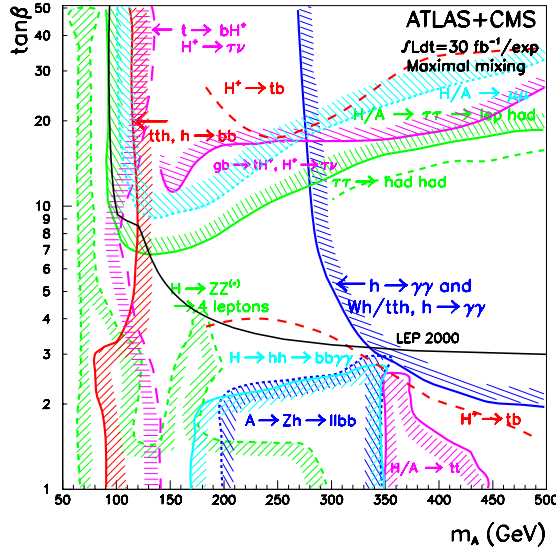


Figure 23: The expected 5σ discovery reach for MSSM Higgses for 30 fb^{-1} per experiment in case of maximal stop mixing[24].

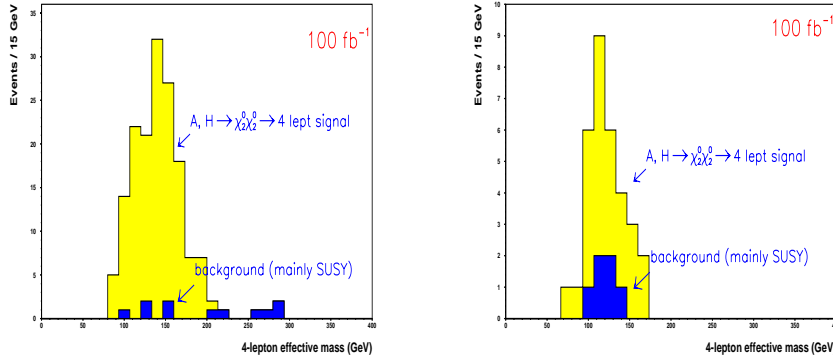


Figure 24: The reconstructed 4 lepton effective mass in $H/A \rightarrow \chi_2^0 \chi_2^0$ decay for $m_A = 320\text{ GeV}$, $\tan\beta = 5$, $M_2 = 120\text{ GeV}$, $M_1 = 60\text{ GeV}$ and $\mu = -500\text{ GeV}$ to the left and $m_A = 380\text{ GeV}$, $\tan\beta = 10$, $M_2 = 180\text{ GeV}$, $M_1 = 100\text{ GeV}$ and $\mu = 500\text{ GeV}$ to the right. In both cases $m_{\tilde{g}} = 250\text{ GeV}$ and $m_{\tilde{q}\tilde{q}} = 1\text{ TeV}$ [27].

the two experiments[24]. For minimal stop mixing, not shown here, the only major change is that the two photon channel is restricted to higher m_A values and the fact that LEP excludes a larger area of the parameter space.

These results are for a constrained choice of SUSY parameters, requiring the SUSY particles to have a mass of $\approx 1\text{ TeV}$. The effect of changing the SUSY particle masses, more specifically of the stop mass, on the Higgs sector has already been illustrated in the $h \rightarrow \gamma\gamma$ channel. Light sparticles may also compete with the SM decay modes of A , H and H^\pm as illustrated in the branching ratios in figures 7, 8 and 9. Figure 24 illustrates the reconstructed 4 lepton effective mass for $H/A \rightarrow \chi_2^0 \chi_2^0 \rightarrow 2\ell\chi_1^0 2\ell\chi_1^0$ for two specific parameters choices[27].

5 What do we learn from the observations?

Discovering Higgs bosons is certainly the primary goal for the LHC experiments, and as shown in previous section, it may well happen in the very first year of LHC running. However, our wish is to understand the nature of electroweak symmetry breaking and only precision measurements of the newly discovered boson can verify the assumptions of the underlying theory.

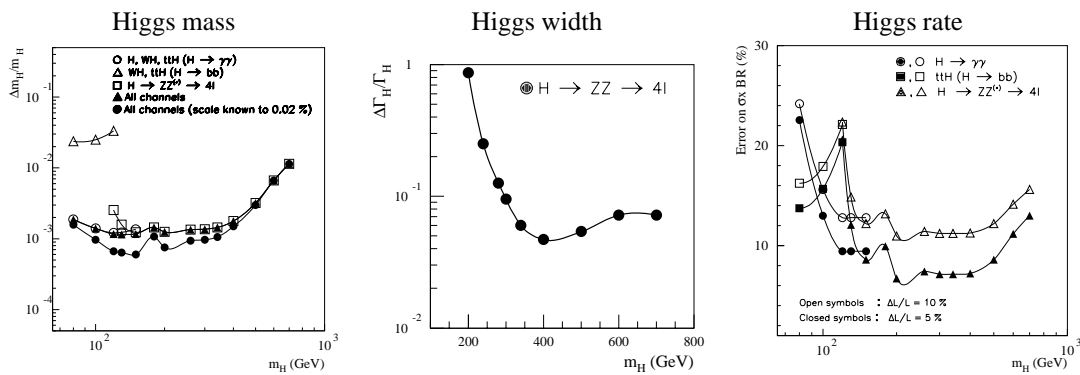


Figure 25: The accuracy in measuring the SM Higgs mass, width and productions rates in ATLAS[16].

5.1 The SM Higgs parameters

The SM model Higgs mass can be determined with an accuracy better than 1% in the two precision channels $H \rightarrow \gamma\gamma$ and $H \rightarrow ZZ \rightarrow 4\ell$ as illustrated in figure 25[16]. The SM width starts to be comparable to the experimental resolution at m_H around 200 GeV and the precision obtained in the measurement of the width is 6% above 300 GeV. The precision of the rate measurements depends on the precision with which the luminosity is known. As shown in figure 25, a precision better than 12% can be obtained in the mass range of $120 \text{ GeV} < m_H < 600 \text{ GeV}$ with a conservative estimate of the luminosity uncertainty (10%).

If no assumptions on the cross-section is made, the experimental data gives the opportunity to determine the couplings and branching ratios by computing the ratios of rates in different production channels. As most of the channels have low rates the determination is dominated by statistical uncertainty and large integrated luminosity is needed for such measurements. However, in these ratios, the luminosity uncertainty cancels.

The $H \rightarrow ZZ^{(*)}$ channel has sensitivity to the Higgs spin in the mass range of $120 \text{ GeV} < m_H < 400 \text{ GeV}$ [28]. It has been suggested[29] that the CP quantum numbers can be verified by studying the angular distribution of jets in the vector boson fusion revealing the tensor structure of HWW coupling.

5.2 The MSSM Higgs parameters

The measurement of the MSSM Higgs sector parameters is even more important as they not only characterise the Higgs bosons themselves but can constrain the other model parameters in the SUSY sector. What can be measured depends clearly on what is discovered. The number of different Higgs bosons observable in the m_A - $\tan\beta$ parameter space is shown in figure 26 for an integrated luminosity of 300 fb^{-1} [24]. In the large $\tan\beta$ region and low $\tan\beta$ region (partly already excluded by the LEP data) several Higgs bosons should be visible. In the intermediate $\tan\beta$ range only the light h is within the discovery reach. Distinguishing the SM and the MSSM in this area will rely on sparticle searches.

The mass measurements of the MSSM Higgs bosons, apart from the masses themselves, give the relations between the MSSM masses, constrained as was shown in figure 1. The rates and widths of the bosons will help to disentangle the SM and the MSSM. An example of a $\tan\beta$ measurement is shown in figure 27[16]. For small $\tan\beta$ its measurement would be possible with rate dependence of the $H \rightarrow ZZ \rightarrow 4\ell$ channel in the small area of the parameter space where it will be visible. For larger value of $\tan\beta$, the rate of the $H \rightarrow \tau\tau$ and $H \rightarrow \mu\mu$ channels is sensitive to $\tan\beta$. The foreseen precision for these channels is shown in figure 27.

6 The first 10 fb^{-1}

The first physics run at the LHC is expected to deliver 10 fb^{-1} of integrated luminosity. This section presents two “case studies”, or rather speculations, on what could be the first signal evidence of the Higgs sector at the LHC.

6.1 $\gamma\gamma$ bump at 120 GeV

Figure 28 shows a hypothetical di-photon distribution in CMS after 10 fb^{-1} . There is a rather little-convincing bump around 120 GeV which, after the subtraction of the background (estimated from the sidebands), becomes a 3.8σ evidence of a 120 GeV Higgs. This should not come as a surprise as the Tevatron, by the LHC start, should

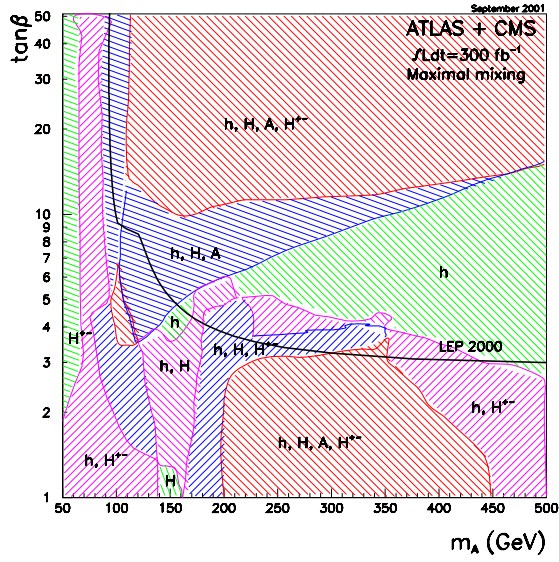


Figure 26: The number of MSSM Higgs bosons within 5σ discovery reach in different regions of the m_A - $\tan\beta$ plane[24].

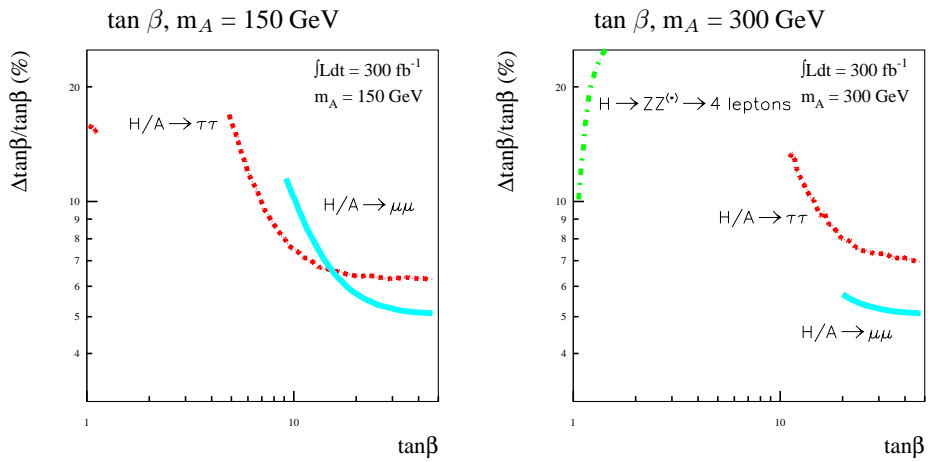


Figure 27: The expected precision on the $\tan\beta$ measurement for 300 fb^{-1} in ATLAS[16].

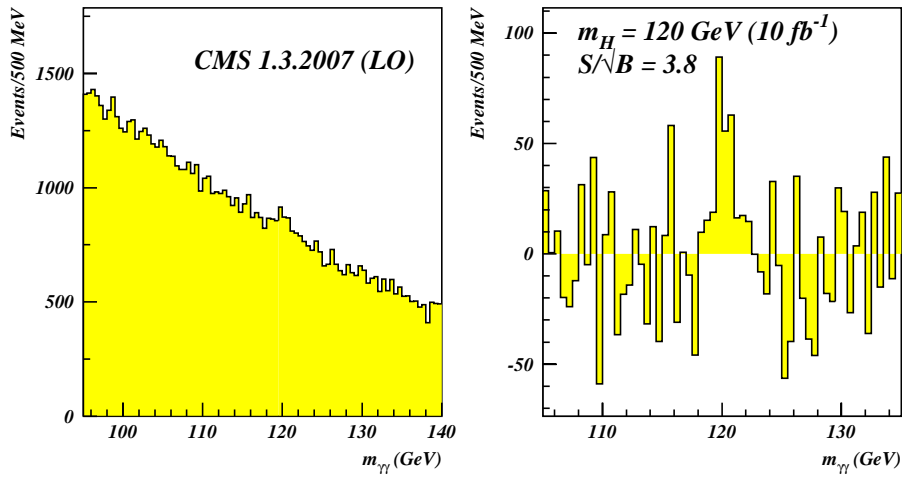


Figure 28: The reconstructed m_H with the background and background subtracted for 10 fb^{-1} .

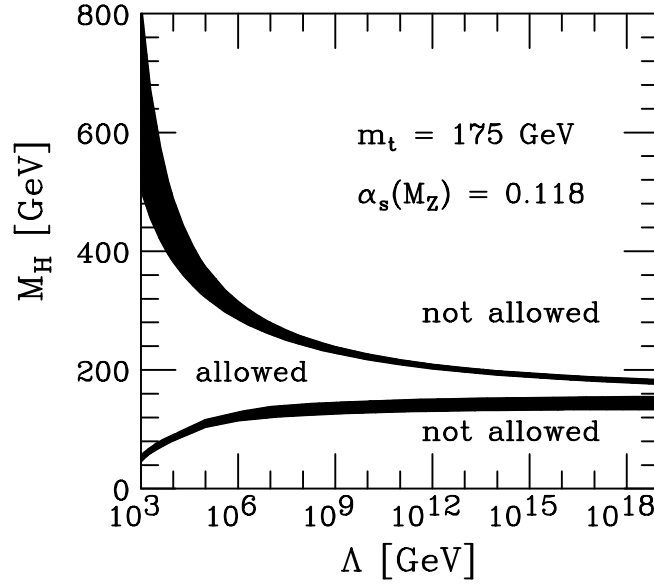


Figure 29: The validity range of the Standard Model versus the Higgs mass[5].

also have given some evidence of it[10]. We can ask what is the impact of such a Higgs on the Standard Model. Figure 29 shows the validity range of the SM as a function of the Higgs mass[5]. The mass of 120 GeV would limit the validity range of the SM model down to 100 – 10 000 TeV, and we can only hope that hints of the new world at such energies propagate down to our observable energy range which will hardly surpass some TeV.

If the observed signal is the light h in the MSSM it is clear that this mass has to be the maximal mass as below it the $\gamma\gamma$ decay would be strongly suppressed. The minimal mixing scenario would be excluded with such a large light h mass. To confirm that the MSSM is indeed the correct model we should wait the $A/H \rightarrow \tau\tau$ to appear if $\tan\beta$ is large enough.

6.2 Excess in $WW \rightarrow \ell\nu\ell\nu$ at 170 GeV

Figure 30 shows the excess in the di-lepton angular distribution for Higgs at $m_H = 170 \text{ GeV}$ decaying into $WW \rightarrow \ell\nu\ell\nu$ with and without the background with 5 fb^{-1} [30]. A clear excess is visible and the 5σ significance limit is already reached. If this excess corresponds to a SM Higgs, the SM could be valid up to the Planck scale as shown in figure 29. The next channel to appear would be $H \rightarrow ZZ^* \rightarrow 4\ell$ and to achieve the 5σ limit for it at this mass would require more than 40 fb^{-1} .

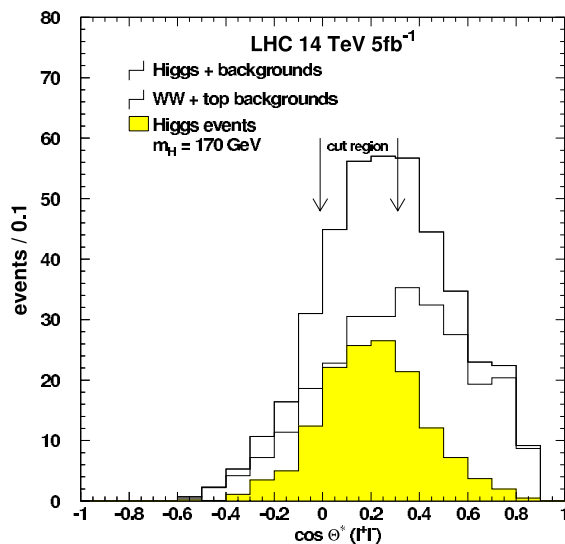


Figure 30: The reconstructed di-lepton angular distribution for the $H \rightarrow WW \rightarrow \ell\nu\ell\nu$ signal and the background[30].

Of the MSSM Higgs candidates, the light h can be excluded as in the MSSM its mass cannot be so large. For the heavy H , the $H \rightarrow WW$ could be visible at low $\tan\beta$. The branching ratio would be $0.5 - 0.7$ at $\tan\beta = 3$ [14]. At low $\tan\beta$, the H production rate is suppressed in comparison with the SM rate. As a consequence, in the case of the MSSM, we would not see as large an excess with as little of integrated luminosity as it is the case in the SM (illustrated in figure 30), but there are chances that this channel is visible as already pointed out in [30]. In this channel, the mass can be measured with ± 5 GeV accuracy, thus giving an estimate of the corresponding $m_A = 150 \pm 10$ GeV as can be estimated from figure 1. Figure 31 shows the area within the 5σ discovery reach for 10 fb^{-1} per experiment[24]. Our H candidate with low $\tan\beta$ and $m_A \approx 150$ GeV could fall in the uncovered area with no other candidates. We could argue that $H \rightarrow WW \rightarrow \ell\nu\ell\nu$ could be used to fill this hole, but systematic study would be needed to confirm this argument. From the correlations between the MSSM Higgs masses we know that the light h should have $m_h \approx 100$ GeV and to confirm that our candidate is a MSSM Higgs we should wait for $h \rightarrow b\bar{b}$ to appear. To have a discovery in the $b\bar{b}$ channel some 60 fb^{-1} needs to be collected.

7 Conclusions

Detailed studies by the ATLAS and CMS collaborations have shown that the SM Higgs searches cover the entire expected mass range, mostly with more than one decay mode for each mass. The low mass range is the most difficult area with the experimentally demanding $H \rightarrow \gamma\gamma$ and $H \rightarrow b\bar{b}$ channels. The SM Higgs profile can be defined with the precision measurements.

In the MSSM, the entire Higgs sector parameter space can be covered with 30 fb^{-1} per experiment. In many areas, several Higgs bosons and decay modes will be available. A significant area can be covered already with 10 fb^{-1} per experiment. Precision measurements in the Higgs sector are possible and can constrain the other parameters of the SUSY model.

The parameter choice for the MSSM physics studies is unavoidably restricted. The aim is to study a presentative set of parameters, and the detector performance and analysis lessons learned from the MSSM studies will serve to explore any non-MSSM scenario.

In conclusion, as elusive as it is now, the Higgs sector will be well known – or well constrained – in seven years from now.

Acknowledgements

This note relies on the enormous amount of work done by my CMS and ATLAS colleagues. I thank especially Daniel Denegri, Sasha Nikitenko, Ritva Kinnunen and Sami Lehti in the CMS collaboration and Fabiola Gianotti, Karl Jakobs and Elzbieta Richter-Was in the ATLAS collaboration for useful advice and for providing the illus-

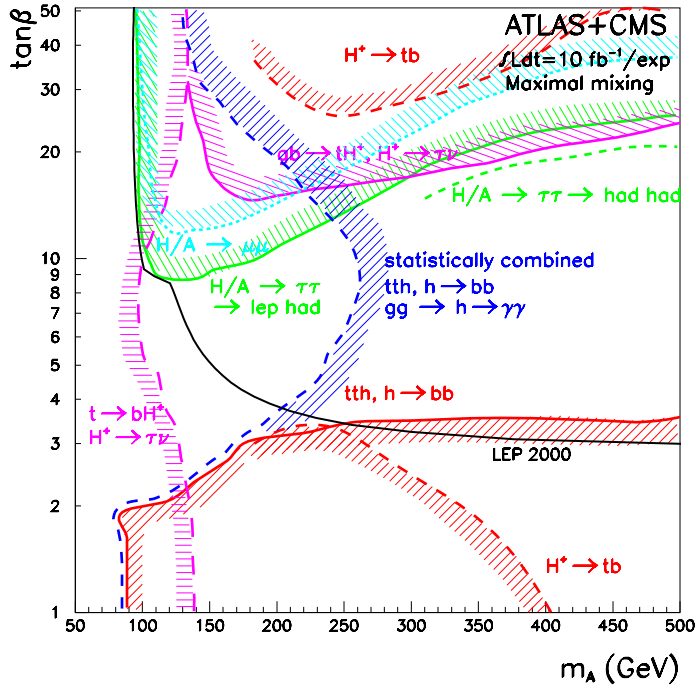


Figure 31: The expected 5σ reach combining 10 fb^{-1} per experiment [24].

trations. I am grateful to Michael Spira with his help with my theoretical doubts and for the use of the HDECAY program and the programs for the Higgs production.

References

- [1] S. Glashow: Nucl. Phys. **22** (1961) 579
S. Weinberg: Phys. Rev. Lett. **19** (1967) 1264
A. Salam in *Elementary Particle Theory*, ed. by N. Svartholm, Aspenäsgråden (1968) 367
- [2] P. Higgs: Phys. Lett. **12** (1964) 132; Phys. Rev. Lett. **113** (1964) 508; Phys. Rev. **1145** (1966) 145
F. Englert and R. Brout: Phys. Rev. Lett. **13** (1964) 321
G. S. Guralnik, C. R. Hagen and T. W. Kibble: Phys. Rev. Lett. **13** (1964) 585
- [3] ATLAS Technical Proposal CERN/LHCC/94-43
- [4] CMS Technical Proposal CERN/LHCC/94-38
- [5] T. Hambye and K. Riesselmann, Phys. Rev. D **55** (1997) 7255
- [6] D. Charlton: BHAM-HEP/01-02 presented in EPS-HEP Budapest, Summer 2001
- [7] The LEP working group for Higgs boson searches: CERN-EP/2001-055
- [8] P. Fayet and S. Ferrara: Phys. Rep. **32** (1977) 249
H. P. Nilles: Phys. Rep. **110** (1984) 1
H. Haber and G. Kane: Phys. Rep. **117** (1985) 75
S. Martin: hep-ph/9709356 (1997)
- [9] H. P. Nilles: Phys. Rep. **110** (1984) 1
S. Dawson: hep-ph/9712464 (1997)
- [10] M. Carena, J. S. Conway, H. E. Haber, J. D. Hobbs: hep-ph/0010338
- [11] The LEP working group for Higgs boson searches: LHWG Note 2001-04

- [12] These programs are available from Michael Spira's website
<http://www.desy.de/~spira/proglist.html>
M. Spira: hep-ph/9510347
- [13] M. Spira: Fortsch. Phys. **46** (1998) 203
- [14] A. Djouadi, J. Kalinowski, M. Spira: Comput. Phys. Commun. **108** (1998) 56
- [15] K. Lassila-Perini: Diss. ETH No. 12961 (1998)
- [16] ATLAS Detector and Physics Performance Technical Design Report CERN/LHCC 99-15
- [17] V. Drollinger, T. Müller, D. Denegri: hep-ph/0111312, CMS Note 2001-054
- [18] A. Nikitenko in Higgs & Supersymmetry Conference, March 19–22, 2001 Orsay
- [19] ATLAS Collaboration, Higgs working group, Oct. 2001, (private communication)
- [20] M. Dittmar: Pramana **55** (2000) 151
- [21] R. Kinnunen et al.: CMS Note 2001-032
- [22] A. Djouadi: Phys. Lett. B **435** (1998) 101
A. Djouadi: hep-ph/9806315
- [23] R. Kinnunen and D. Denegri: CMS Note 1999-037
- [24] ATLAS Detector and Physics Performance Technical Design Report CERN/LHCC 99-15
ATLAS Higgs Working Group
- [25] S. Lehti: Dissertation, University of Helsinki, Report Series in Physics, HU-P-D93,2001
- [26] R. Kinnunen: CMS Note 2000-045
- [27] F. Moortgat: CMS CR 2001-005
- [28] M. Hohlfeld: ATL-PHYS-2001-004
- [29] D. Zeppenfeld in Physics at TeV Colliders II workshop, May 21 – June 1, 2001, Les Houches
- [30] M. Dittmar, H. Dreiner: Phys. Rev. D **55**, (1997) 167